NANO LETTERS

2009
Vol. 9, No. 12
4037-4041

Incomplete Exciton Harvesting from Fullerenes in Bulk Heterojunction Solar Cells

George F. Burkhard,[†] Eric T. Hoke,[†] Shawn R. Scully,[‡] and Michael D. McGehee*,[‡]

Department of Applied Physics and Department of Materials Science and Engineering, Stanford University, Stanford, California 94305

Received July 9, 2009; Revised Manuscript Received September 13, 2009

ABSTRACT

We investigate the internal quantum efficiencies (IQEs) of high efficiency poly-3-hexylthiophene:[6,6]-phenyl-C_{61}-butyric acid methyl ester (P3HT:PCBM) solar cells and find them to be lower at wavelengths where the PCBM absorbs. Because the exciton diffusion length in PCBM is too small, excitons generated in PCBM decay before reaching the donor−acceptor interface. This result has implications for most state of the art organic solar cells, since all of the most efficient devices use fullerenes as electron acceptors.

Since their inception, organic photovoltaics (OPVs) have steadily improved in performance. OPVs generate power through three major processes: exciton generation (absorption), exciton harvesting (the process of excitons migrating to the donor/acceptor interface and being split into their constituent charges), and charge transport.[1,2] A typical device consists of a charge generating active layer sandwiched between hole extracting and electron extracting electrodes. The active layer consists of an electron-donating material in contact with an electron-accepting material. Excitons, bound electron−hole pairs, are generated when light is absorbed in one of the materials. If an exciton is sufficiently close to the donor/acceptor interface, the exciton is split into its constituent charges, leaving an electron in the acceptor and a hole in the donor. Today's best OPVs are made with active layers using a bulk heterojunction structure obtained by blending a polymer donor with a fullerene acceptor.[3−5] In bulk heterojunction solar cells, the donor and acceptor are naturally nanostructured due to phase segregation of the polymer and fullerene. The morphology of the nanostructure is somewhat tunable through thermal and solvent annealing. Annealing typically increases the size of the domains in the blend, which increases the distance excitons need to travel to dissociate at the heterojunction interface. The increase in domain size also affects charge carrier mobilities and therefore the recombination mechanisms in the devices.[6] Optimized devices have power conversion efficiencies of 5−6%.[4,5,7] Pushing these efficiencies higher requires detailed analysis of the losses in these devices. A fraction of the excitons in most pure materials decay radiatively, so exciton harvesting is usually evaluated by observing photoluminescence quenching. In C_{60} fullerene systems like poly-3-hexylthiophene:[6,6]-phenyl-C_{61}-butyric acid methyl ester (P3HT:PCBM), the PCBM emission is extremely weak and its emission spectrum overlaps that of the polymer, so this technique can only effectively probe exciton quenching in the polymer phase. Most analyses assume the overall exciton harvesting efficiency to be very close to 100%.[8−10] In this paper we show that for the highest efficiency P3HT:PCBM cells, the internal quantum efficiency is lower at wavelengths where the PCBM absorbs. We find that the exciton harvesting in the fullerene phase is less than 50% efficient. While absorption in the fullerene is weak compared to the polymer, recovering this loss would increase the photocurrent by 7−8%.

External quantum efficiency (EQE), the ratio of charges extracted from a device to the number of incident photons is an important benchmark of solar cell performance. Figure 1a shows the EQE and absorption of a typical high performance (power conversion efficiency >4%) P3HT:PCBM solar cell used in this study and is consistent with EQE spectra of high efficiency cells published in the literature.[4,6,11] Internal quantum efficiency, the ratio of charges extracted from a device to the number of photons absorbed by the active layer, provides a useful way to isolate electronic loss mechanisms from light coupling and parasitic absorption losses in a solar cell. The top curve in Figure 1b shows a typical IQE spectrum for the same high efficiency P3HT:PCBM devices. We found that the IQE curves were far from flat; the IQE ranges from 50 to 75%, with lower IQE at shorter wavelengths. Because more of the short-

* Corresponding author, mmcgehee@stanford.edu.
[†] Department of Applied Physics.
[‡] Department of Materials Science and Engineering.

10.1021/nl902205n CCC: $40.75
Published on Web 10/07/2009

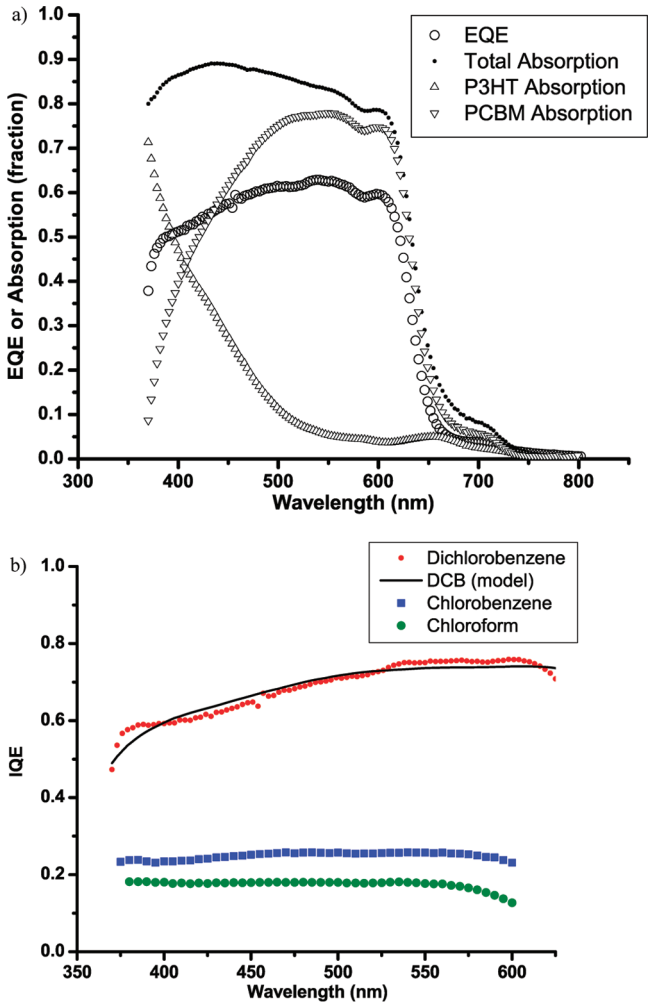

Figure 1. (a) Experimentally measured EQE and absorption of a P3HT:PCBM cell cast from 1,2-dichlorobenzene (solvent and thermally annealed). The absorption in the active layer was extracted from the total absorption using a transfer matrix optical model. The contributions of the P3HT and PCBM to the active layer absorption were determined by multiplying the active layer absorption by the ratio of each component's imaginary index of refraction to the total imaginary index of refraction of the blend. (b) Experimentally measured IQE curves of P3HT:PCBM cells cast from 1,2-dichlorobenzene (solvent and thermally annealed), chlorobenzene (as cast), and chloroform (as cast) as well as modeled IQE for the dichlorobenzene cell.

wavelength absorption occurs in the PCBM, the low IQE in this region suggests that not all excitons generated in the PCBM are harvested.

The IQE can be factored into three distinct parts: exciton diffusion, charge transfer, and charge collection.

$$\eta_{IQE} = \eta_{ED}\eta_{CT}\eta_{CC} \tag{1}$$

Each of these terms can have wavelength dependence. Exciton diffusion and charge transfer are processes that involve excitons in either the donor or the acceptor phase and therefore might have different efficiencies depending on the properties of the phase in question. Such differences would result in wavelength dependence of the exciton diffusion and charge transfer efficiencies since the absorption contribution and thus exciton generation contribution of each of the phases changes with wavelength. Effects that generate multiple excitons from a single photon could also result in wavelength-dependent exciton diffusion and charge transfer efficiencies; however these effects have not been observed in polymer−fullerene blend systems. Charge collection encompasses all of the transport processes involved in moving electrons and holes to their respective electrodes and includes geminate and bimolecular recombination. The charge collection process begins after excitons are split at the heterojunction interface and is therefore insensitive to the exciton's origin; the charge collection process always begins with an electron in the acceptor and a hole in the donor. The charge collection efficiency, however, can vary with position in the device due to differences in distances the charges need to travel to be extracted, variations in morphology, or interactions with electrodes. Optical interference effects cause exciton generation profiles for different wavelengths of light to have maxima at different locations in the device. When combined, these two effects can lead to wavelength dependence of the charge collection efficiency. In a device where the exciton diffusion and charge transfer efficiencies are equal in both materials, and the charge transport efficiency does not change much throughout its thickness, the IQE should be independent of excitation wavelength.

To allow for different exciton diffusion and charge efficiencies for the donor and acceptor materials, we modeled the IQE with the equation

$$IQE = \frac{\eta_{CC}(x)(\eta_D Abs_D(\lambda) + \eta_A Abs_A(\lambda))}{Abs_D(\lambda) + Abs_A(\lambda)} \tag{2}$$

where Abs_D and Abs_A are the contributions to the absorption spectrum and η_D and η_A are the exciton harvesting efficiencies $\eta_{ED}\eta_{CT}$ of the donor and acceptor, respectively. Note that the numerator corresponds to the external quantum efficiency and the denominator corresponds to the total absorption in the active layer. Abs_D and Abs_A were determined by measuring the total reflectance of the device and deriving from this the absorption of the active layer using a transfer matrix optical model.[1,12] The absorption due to either component in the blend was then calculated by multiplying the active layer absorption by the ratio of the k value (the imaginary part of the complex index of refraction) in question to the total k at the wavelength of interest

$$Abs_{P3HT} = Abs_{ActiveLayer}\frac{k_{P3HT}}{k_{P3HT} + k_{PCBM}} \tag{3}$$

Further details on these measurements are provided at the end of this paper and in the Supporting Information.

The top curves in Figure 1b show the fit between the modeled and experimental IQE. Figure 1a shows the experimentally measured EQE and absorption data used to generate the IQE curve. The best fit of eq 2 to the IQE curve in Figure 1b is obtained by taking $\eta_{CC} = 79 +1/-4\%$, $\eta_D =$

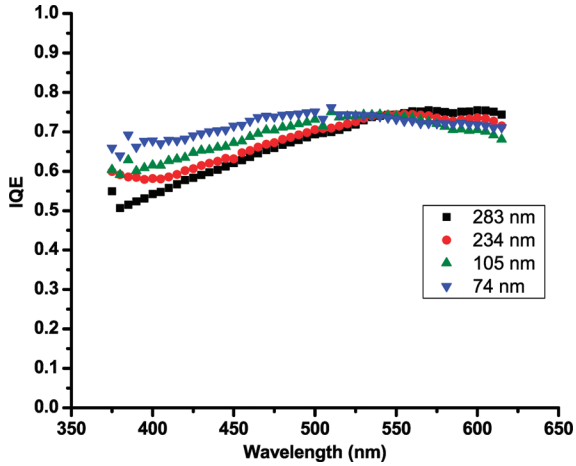

Figure 2. IQE curves for devices of varying active layer thickness. These devices were processed in the same manner as the high-efficiency device shown as the top curve in Figure 1a.

95 +5/−2%, and η_A = 41 +5/−1%. These are standard errors and represent the extreme values the fit parameters could take at the 50% confidence level assuming a normal distribution of error. The fit value for exciton harvesting in the donor, η_D = 95%, is consistent with photoluminescence measurements which show 95% quenching of the emissive excitons.

The observation that only 41% of excitons in PCBM are harvested indicates either that the diffusion length is smaller than the PCBM domain size or that there is some other excitation decay pathway. If the former is true, then by reducing the domain size we should be able to recover all of the excitons lost in the PCBM. Modeling the system with $\eta_A = \eta_D$ = 95% suggests that if all of the PCBM excitons were harvested, we would see an increase in the photocurrent of 7−8%.

To probe the dependence of exciton harvesting on domain size, we created blends cast from lower boiling point solvents (chloroform and chlorobenzene) without annealing to ensure that the domains were as small as possible. As seen in the two lower curves in Figure 1b, the IQEs of these devices are independent of wavelength, indicating that both the PCBM and P3HT have high exciton harvesting efficiencies. Of course the IQE is also low, indicating that while shrinking the domains improved exciton harvesting, it dramatically decreased the charge transport efficiency, making the device less efficient overall.

We considered the possibility that the wavelength dependence of the IQE could be due to variations in η_{CC} from optical interference effects. If this were the case, we would expect to see IQE minima at different wavelengths for devices of different thicknesses. However, we observed that the minimum IQE is always in the blue end of the spectrum (Figure 2). This implies that the charge collection has negligible dependence on excitation wavelength. We also considered the possibility that singlets generated in the PCBM might be lost via mechanisms other than internal conversion, such as energy transfer to polarons[13−15] or intersystem crossing to the triplet state.[16] It is possible that triplets have lower charge separation efficiency due to their lower energy; however, the fact that we were able to recover these excitons by making the PCBM domains smaller points to exciton diffusion rather than charge separation as the reason for the reduced IQE. Additionally, the IQE curves are independent of excitation intensity up to one sun (data not shown), which discounts energy transfer to polarons since this recombination pathway depends on the carrier density.

The exciton diffusion lengths in PCBM have not yet been thoroughly studied; however, Cook et al. have performed measurements that suggest a value as small as 5 nm.[17] We have not measured the exciton diffusion length because most methods for doing so detect photoluminescence quenching and PCBM is a very weak emitter. Furthermore any technique that analyzed thin films of pure PCBM might not reveal the exciton diffusion length for PCBM in a bulk heterojunction due to differences in morphology. PCBM domain sizes vary and are typically 10−100 nm after annealing for 5 min at 100 °C[18] and up to tens of micrometers after annealing at higher temperatures for longer periods of time.[19] It is therefore not surprising that the domains might be significantly larger than the exciton diffusion length.

Incomplete exciton harvesting from fullerenes might help explain some effects seen by others. Moulé et al. observed a "reduced generation zone" (RGZ) in the active layer near the poly(3,4-ethylenedioxythiophene):poly(styrenesulfonate) (PEDOT:PSS) interface.[20] Several studies have shown vertical phase segregation of the active layer,[3,21] where larger fullerene domains lie near this interface. This could be due to the more polar nature of PCBM compared with P3HT[22−25] or because PCBM is more soluble than the polymer in the casting solvent, which evaporates from the top surface first. These studies used multiple characterization techniques including ellipsometry, near-edge X-ray absorption fine structure spectroscopy, dynamic secondary ion mass spectroscopy, and energy compatibility arguments. Our data are consistent with the hypothesis that the observed RGZ is due to excitonic losses in the fullerene due to the larger domain size near the active layer/PEDOT boundary. Having less polymer at this interface would also weaken absorption in this area, reducing generation; however this would not explain the wavelength dependence of the IQE we observe. Figure 2 shows IQE curves for devices made in the same manner as the high-efficiency cells but with active layers of varying thickness. We observed that while all of the cells had similar IQEs at longer wavelengths, thinner cells generally had higher IQEs at shorter wavelengths than thicker cells. This is consistent with a vertical phase segregation model where the largest PCBM domains appear close to the PEDOT interface. TEM tomography has suggested that vertical phase segregation occurs with the opposite orientation (PCBM accumulating near the metal electrode).[26] A thorough discussion of this is beyond the scope of this paper; however, we note that TEM methods can only differentiate PCBM from *crystalline* P3HT. Thus, the TEM data could be interpreted to mean that there is more polymer at the PEDOT interface or that the P3HT is more crystalline in this region. While the general effect of vertical phase

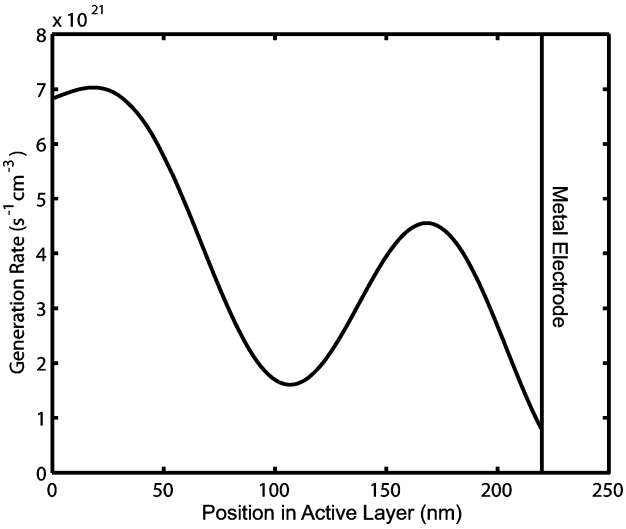

Figure 3. Exciton generation rate in the active layer vs position in the device for an optimized (220 nm active layer thickness) under AM1.5G illumination. The left side of the plot (0 nm) represents the interface with the PEDOT; the right boundary (220 nm) represents the boundary with the reflective metal electrode.

segregation would be that thicker films will show a larger fraction of oversized PCBM domains, this effect might be especially important for the thick films used to make high efficiency solar cells. Optical interference modeling, shown in Figure 3, confirms that for these cells (optimized to 220 nm active layer thickness), the highest excitation rates occur near this interface. It should be noted that solvent and thermal annealing of the blend results in larger PCBM domains throughout the film, so we would predict poorer exciton harvesting in the PCBM phase regardless of vertical phase segregation.

Park et al. recently published work on a 6.1% efficient cell using poly[*N*-900-hepta-decanyl-2,7-carbazole-*alt*-5,5-(40,70-di-2-thienyl-20,10,30-benzothiadiazole) (PCDTBT) as a donor material that does not require long periods of solvent or thermal annealing to achieve good device performance[5] and does not suffer from an exciton harvesting problem in the fullerene, as evidenced by their flat, near-100% IQE. Their device uses a very thin (80 nm) active layer. Because charge carriers have less far to travel, mobility requirements are less stringent and annealing is not required for good device performance. Because they do not anneal their films, the donor and acceptor are probably more intimately mixed. If this is true, it might explain why their exciton harvesting efficiency is very close to 100% for both the polymer and the fullerene. Their high, flat IQE shows that the exciton harvesting problem is not an insurmountable one and that better design rules are enough to make higher efficiency organic solar cells.

We used IQE measurements as a tool to investigate exciton harvesting efficiencies in P3HT:PCBM bulk heterojunction solar cells and found that in the best performing cells with high electron and hole mobilities, there is incomplete harvesting of excitons in the fullerene phase. The exciton diffusion length in the fullerene is generally shorter than the domain size, and approximately 60% of excitons generated in the fullerene phase decay before being harvested. We are currently investigating the same effect in devices made with $PC_{70}BM$, which absorbs more strongly in the solar spectrum. Preliminary results indicate that these devices have a similar exciton harvesting issue; however quantitative analysis is still underway. Our findings have implications for most bulk heterojunction solar cells since the vast majority use PCBM as an electron acceptor. Novel geometries that use strongly absorbing, thin active layers may bypass this issue by using blends with smaller domains since having high charge carrier mobilities is less important in a thinner device. It may also be possible to solve this problem in more standard devices using novel nanostructures or new acceptors.

Devices were made with the structure indium tin oxide (ITO)/PEDOT:PSS/P3HT:PCBM/Ca/Al with the following thicknesses (in nm): 110/35/220/7/200. ITO substrates were purchased from Sorizon Technologies, PEDOT:PSS from Baytron, P3HT from Rieke, PCBM from NanoC, and metals from K. J. Lesker. Substrates were cleaned in an ultrasonic bath with Extran 300, rinsed in deionized water, and then cleaned in acetone and 2-propanol followed by 20 min of UV−ozone treatment. PEDOT:PSS was spin-coated and the substrates were annealed at 140 °C for 10 min. They were then transferred to a nitrogen glovebox, where they remained for the duration of the fabrication process as well as for all characterizations performed. P3HT:PCBM (1:1 ratio by weight) was cast from 1,2-dichlorobenzene, chlorobenzene, or chloroform. The devices cast from dichlorobenzene were allowed to slow-dry overnight and were thermally annealed at 110 °C for 10 min. Calcium and aluminum metal electrodes were deposited in a thermal evaporator.

IQE was calculated using an external quantum efficiency (EQE) measurement as well as a reflection-mode absorption measurement. EQE was taken at short circuit using monochromated white light from a tungsten lamp. EQE was calculated by comparing the photocurrent action spectrum of the device to that of a NIST traceable calibration photodiode. The device absorption spectrum was measured in reflection mode inside of an integrating sphere (to capture scattered light) using the same monochromated white light source and calibrated photodiode. Parasitic absorption in the ITO, PEDOT, and metals was calculated using a transfer matrix formalism[1,12] to evaluate the coherent superposition of light waves at each interface which is described in the Supporting Information. The active layer absorption was then calculated by subtracting the modeled parasitic absorption from the experimentally measured total absorption. Indices of refraction for the various materials were either taken from literature[2] or measured using a combination of spectroscopic ellipsometry and absorption/reflection measurements.

Acknowledgment. This work was supported by the Center for Advanced Molecular Photovoltaics (Award No KUS-C1-015-21), made by King Abdullah University of Science and Technology (KAUST) and partially by the Global Climate Energy Project (GCEP). E.T.H. is supported by the National Science Foundation GRFP and the Fannie and John Hertz Foundation.

Supporting Information Available: Calculating Abs_D and Abs_A and a typical comparison of calculated total reflectance vs experimentally measured reflectance. This material is available free of charge via the Internet at http://pubs.acs.org.

References

(1) Peumans, P.; Yakimov, A.; Forrest, S. *J. Appl. Phys.* **2003**, *93*, 3693–3723.
(2) Kotlarski, J. D.; Blom, P. W. M.; Koster, L. J. A.; Lenes, M.; Slooff, L. H. *J. Appl. Phys.* **2008**, *103*, 084502.
(3) Li, G.; Shrotriya, V.; Huang, J. S.; Yao, Y.; Moriarty, T.; Emery, K.; Yang, Y. *Nat. Mater.* **2005**, *4* (11), 864–868.
(4) Peet, J.; Kim, J. Y.; Coates, N. E.; Ma, W. L.; Moses, D.; Heeger, A. J.; Bazan, G. C. *Nat. Mater.* **2007**, *6* (7), 497–500.
(5) Park, S. H.; Roy, A.; Beaupre, S.; Cho, S.; Coates, N.; Moon, J. S.; Moses, D.; Leclerc, M.; Lee, K.; Heeger, A. J. *Nat. Photonics* **2009**, *3* (5), 297–302.
(6) Li, G.; Yao, Y.; Yang, H.; Shrotriya, V.; Yang, G.; Yang, Y. *Adv. Funct. Mater.* **2007**, *17*, 1636–1644.
(7) Kim, Y.; Cook, S.; Tuladhar, S. M.; Choulis, S. A.; Nelson, J.; Durrant, J. R.; Bradley, D. D. C.; Giles, M.; McCulloch, I.; Ha, C.-S.; Ree, M. *Nat. Mater.* **2006**, *5*, 197–203.
(8) Mayer, A. C.; Scully, S. R.; Hardin, B. E.; Rowell, M. W.; McGehee, M. D. *Mater. Today* **2007**, 28–33.
(9) Yang, X.; Loos, J. *Macromolecules* **2007**, *40* (5), 1353–1362.
(10) Dennler, G.; Scharber, M. C.; Brabec, C. J. *Adv. Mater.* **2009**, *21*, 1323–1338.
(11) Dennler, G.; Forberich, K.; Scharber, M. C.; Brabec, C. J.; Tomiš, I.; Hingerl, K.; Fromherz, T. *J. Appl. Phys.* **2007**, *102*, 054516.
(12) Pettersson, L. A. A.; Roman, L. S.; Inganas, O. *J. Appl. Phys.* **1999**, *86* (1), 487–496.
(13) Scully, S. R.; McGehee, M. D. *J. Appl. Phys.* **2006**, *100* (3), 034907.
(14) Liu, Y. X.; Summers, M. A.; Scully, S. R.; McGehee, M. D. *J. Appl. Phys.* **2006**, *99*, 093521.
(15) Hukka, T. I.; Toivonen, T.; Hennebicq, E.; Bredas, J. L.; Janssen, R. A. J.; Beljonne, D. *Adv. Mater.* **2006**, *18* (10), 1301–1306.
(16) Cook, S.; Durrant, J. R. *Chem. Phys. Lett.* **2007**, *445* (4−6), 276–280.
(17) Cook, S.; Furube, A.; Katoh, R.; Han, L. *Chem. Phys. Lett.* **2009**, doi: 10.1016/j.cplett.2009.06.091.
(18) Vanlaeke, P.; Swinnen, A.; Haeldermans, I.; Vanhoyland, G.; Aernouts, T.; Cheyns, D.; Deibel, C.; D'Haen, J.; Heremans, P.; Poortmans, J.; Manca, J. V. *Sol. Energy Mater. Sol. Cells* **2006**, (90), 2150–2158.
(19) Savenije, T. J.; Kroeze, J. E.; Yang, X. N.; Loos, J. *Adv. Funct. Mater.* **2005**, *15* (8), 1260–1266.
(20) Moulé, A. J.; Meerholz, K. *Appl. Phys. B: Laser Opt.* **2009**, *92*, 209–218.
(21) Yang, X. N.; Loos, J.; Veenstra, S. C.; Verhees, W. J. H.; Wienk, M. M.; Kroon, J. M.; Michels, M. A. J.; Janssen, R. A. J. *Nano Lett.* **2005**, *5* (4), 579–583.
(22) Campoy-Quiles, M.; Ferenczi, T.; Agostinelli, T.; Etchegoin, P. G.; Kim, Y.; Anthopoulos, T. D.; Stavrinou, P. N.; Bradley, D. D. C.; Nelson, J. *Nat. Mater.* **2008**, *7*, 158–164.
(23) Germack, D. S.; Chan, C. K.; Hamadani, B. H.; Richter, L. J.; Fischer, D. A.; Gundlach, D. J.; DeLongchamp, D. M. *Appl. Phys. Lett.* **2009**, *94*, 233303.
(24) Björström, C. M.; Bernasik, A.; Rysz, J.; Budkowski, A.; Nilsson, S.; Svensson, M.; Andersson, M. R.; Magnusson, K. O.; Moons, E. *J. Phys.: Condens. Matter* **2005**, *17*, L529–L534.
(25) Barrau, S.; Andersson, V.; Zhang, F.; Masich, S.; Bijleveld, J.; Andersson, M. R.; Inganäs, O. *Macromolecules* **2009**, *42* (13), 4646–4650.
(26) van Bavel, S. S.; Sourty, E.; With, G. d.; Loos, J. *Nano Lett.* **2009**, *9* (2), 507–513.

NL902205N